Proceedings of ASME Turbo Expo 2011
GT2011
June 6-10, 2011, Vancouver, British Columbia, Canada

GT2011-46183

LOWERING EQUIVALENCE RATIO LIMIT FOR STABLE COMBUSTION IN GAS TURBINES BY INJECTION OF FREE RADICALS

Yeshayahou Levy, Vladimir Erenburg, Valery Sherbaum, Vitaly Ovcharenko, Leonid Rosentsvit
Faculty of Aerospace Engineering, Technion, Israel Institute of Technology

Boris Chudnovsky, Amiel Herszage, Alexander Talanker
Israel Electric Company

ABSTRACT

Lean premixed combustion is one of the widely used methods for NO_x reduction in gas turbines (GT). When this method is used combustion takes place under low Equivalence Ratio (ER) and at relatively low combustion temperature. While reducing temperature decreases NO_X formation, lowering temperature reduces the reaction rate of the hydrocarbon–oxygen reactions and deteriorates combustion stability. The objective of the present work was to study the possibility to decrease the lower limit of the stable combustion regime by the injection of free radicals into the combustion zone.

A lean premixed gaseous combustor was designed to include a circumferential concentric pilot flame. The pilot combustor operates under rich fuel to air ratio, therefore it generates a significant amount of reactive radicals.

The experiments as well as CFD and CHEMKIN simulations showed that despite of the high temperatures obtained in the vicinity of the pilot ring, the radicals' injection from the pilot combustor has the potential to lower the limit of the global ER (and temperatures) while maintaining stable combustion. Spectrometric measurements along the combustor showed that the fuel-rich pilot flame generates free radicals that augment combustion stability.

In order to study the relevant mechanisms responsible for combustion stabilization, CHEMKIN simulations were performed. The developed chemical network model took into account some of the basic parameters of the combustion process: ER, residence time, and the distribution of the reactances along the combustor. The CHEMKIN simulations showed satisfactory agreement with experimental results.

Introduction

The regulatory requirements for low emissions from gas turbine power plants have increased during recent years. Environmental agencies throughout the world are now requiring even lower rates of emissions of NOx and other pollutants from both, new and existing gas turbines. Traditional methods of reducing NOx emissions from combustion turbines (water and steam injection) are limited in their ability to reach the extremely low levels, as required by many municipal authorities. As known, the rate of NO_x production dramatically decreases as flame temperature is reduced. This is because of the exponential effect of temperature on NO_x production as described, for example, by the Zeldovich Mechanism; and this is the reason why injection of coolants or diluents (usually water or steam) into the flame zone of gas turbine combustor reduces NO_x emissions. For the same reason, very lean dry combustors can be used to control emissions [1]. There are two design challenges associated with very lean combustors. First, care must be taken to ensure that the flame is stable at the design operating point. Second, a turndown capability is necessary since a gas turbine must be able to start (ignite), accelerate, and operate over the load range. Both of these challenges are driven by the need to operate the combustor at low flame temperatures, to achieve very low emissions. Therefore the combustor operation at full load is just above the flame blowout point, which is the point at which combustion of a premixed fuel and air mixture is unable to self-sustain. At lower loads the ER may reduce as well so will the associated flame temperature thus approaching the blowout conditions. Eventually, at some point the flame will either become unstable (with associated pressure oscillations) or even blow out [2-5]. Clearly the latter oscillations are, to some extent, related to the combustion chamber geometry and flow properties that determine the rendered standing waves pattern. Interestingly, leaving aside the influence of the above mentioned variables, the very lean character of the mixture appears to play an important role on the stability boundaries.

Experimental results [4] reveal that the magnitude of a longitudinal acoustic disturbance grows with decreasing ER, until it eventually initiates a lower-frequency, high-amplitude instability. This low-frequency instability is visible as a flapping of the flame and augments severity with decreasing ER until it induces combustion blowout. It can be assumed that if the lean blowout limit could be lowered, the acoustic stability range could be broadened. Such assumption has been confirmed by an experimental study [5], where Albrecht et al showed in their study that boundaries of stability and blowout limits are almost parallel to one another. This result did not depend on equivalence ratio and blowout limit was 60-100 K degrees below that of stability limit; i.e. this result confirms our assumption that there is a link between combustion instability and blowout. The above described behavior is in direct contrast to that of a diffusion flame combustor. In diffusion type of combustor, the fuel is injected, mixed and burns at stoichiometric (maximum) flame temperature using only a portion of the available air (as diffusion or partially premixed combustion system). Such regime results in high NOx emissions, but has the benefit of very good stability because the flame burns always at nearly the same high temperature, almost independent of fuel flow. In response to these challenges, combustion system designers use combustors in which one section of the flame zone is designed as a diffusion flame, and another section as a lean premixed zone. Thus the combustion may be distributed into two zones with different ER. Typically, it is necessary to maintain stable combustion also at lower loads or during startup. This may be achieved by different fuel distributions in the different combustion zones of the combustor.

Several stability control techniques have already been investigated and developed. As it is noted in [6], pilot flames can alleviate stability. This is done either by minimizing dynamic instability or by sustaining the main combustion process at operating points where instabilities are otherwise likely to occur. In their study, Albrecht et al. [6], investigated the effect of two different premixed pilot injectors on the combustion stability. One of the pilot flame injector was located upstream of the recirculation zone at the apex of the burner. The second one was a pilot ring placed at the burner outlet on the dump plane. The investigation showed that these premixed pilot flames were able to suppress instabilities over a wider fuel/air ratio range than the conventional premixed pilot injection alone. Furthermore, when a certain percentage of the fuel was premixed with air and injected through the pilot ring, it was possible to prevent instabilities and maintain stable flame near the lean blowout. Consequently, NOx emissions were significantly reduced. The use of a hydrogen torch has shown improvement in the lean-stability limit in GT's LP combustion systems. Also, it was shown experimentally [7] that hydrogen jet injection into a premixed propane flame breaks the coupling between acoustic and heat release oscillations and result in a significant decrease in the amplitude of the pressure oscillations, while the heat release oscillations remain at the same level. Another experimental investigation, [5], on combustion of hydrogen-enriched methane/natural gas in a LP swirl-stabilized burner, showed that the lean stability and blowout limits were lowered. It was also found that the use of hydrogen blended fuel, significantly reduced CO emissions, without adversely affecting the NO_X emissions.

A numerical study on the effect of addition of high radical concentration $\left(>0.1\%\right)$ to a hydrogen/air flame [8] demonstrated an increase in burning velocity and a decrease in ignition delay time at temperatures higher than 750K. It was claimed in an experimental study of pre-chamber ignition [9] that the residence time $\left(t_{res}=2-9\ m\sec\right)$ for rich mixtures $\left(\phi=1.25\right)$ is comparable to the active atoms' and radicals' life time $\left(\approx 10\ m\sec\right)$, and the experiments confirmed the chemical activity of rich mixture combustion products. Similar results were achieved in studies [10-12]. Consequently, it can be deduced that pre-chamber radicals' injection bears great potential in stabilizing and enhancing LP flames.

The objectives of the present study are;

- To analyze the mechanism how injection of free radicals affects combustion process;
- To study evolution of free radical along a combustor;
- To find optimal ER of the injected fuel.

For this purpose, CFD and CHEMKIN simulations were carried out. In parallel, experimental study included analysis of combustion products and spectroscopic measurements of the chemiluminescence from the combustion gases. Results are supposed to improve knowledge associated with the augmentation of combustion stability by radical injection.

CFD Model

CFD simulations were used as a basis for the CHEMKIN model and for design of final shape of the combustor unit. The specific design was realized by adopting a tubular design without a primary zone. Detailed description of the chosen model is given in [2]. The longitudinal section of the combustor unit geometry is shown in Fig. 1. The air was delivered to combustor through a 52 mm diameter tube. Gas was delivered through a 15 mm diameter tube which was located at the center of air tube. Six radial nozzles with orifice diameter of 1 mm were located in the gas tube at an angle of 45 degrees relative to the tube axis for the distribution and mixing the gas in the air. To provide good pre-mixing with air, the nozzles were located at the distance 50 mm upstream the combustor. Combustor diameter was 90 mm. Combustion products from the pilot combustor are delivered to the main combustor through an annular slot upstream of the conical section of the combustor. In order to determine the exact shape of the conical section, CFD simulations were performed for a sudden expansion combustor configuration. The purpose of the simulations was to identify the recirculation region in the sudden expansion combustor and to determine its dimensions and the associated contour of the zero velocity line separating the recirculation bubble from the main flow. Once the zero velocity line is identified, it was copied to be used as the contour of the conical section in the experimental combustor. Such an analogy was adopted to verify the ability of the pilot ring combustor to act as the replacement for the stabilization mechanism of the step in the sudden expansion (dump) combustor. In the actual design the region of sudden expansion was replaced by cone with an angle that equaled to 11^0. Propane/butane gas was used in the tests.

Each burner unit received the following inlet flow rates:

1. Pilot combustor air: m_{pa}=0.4 g/s.
2. Pilot combustor fuel m_{pf}=0.03 g/s.
3. Main combustor m_{ma}=32.5 g/s
4. Main combustor fuel m_{mf}=0.9 g/s

The model is based on the solution of the momentum and energy equations, and an additional transport equation for the solution of the so called reaction progress variable (RPV), c. This variable is defined as the density averaged value of the ratio between the sum of the mass fractions of the different combustion products species, Y_i and their sum after complete adiabatic combustion. Hence, c will adopt the value $c = 0$ where the mixture is un-burnt and $c = 1$ where the mixture is burnt.

Contours of fuel concentrations enable to follow the progress of the combustion process inside the combustion region. This region increases along the combustor. As mentioned above, the numerical results are based on a single reaction mechanism. Nevertheless, they provide a basis which enables to describe the combustion process in general and gives useful initial information for the CHEMKIN simulation: the length of the combustion zone is equal to approximately 10 diameters of air inlet; as the distance from the inlet increases, the width of this zone also increases. Part of the combustion products do not participate in the combustion process after burning – which means that fresh fuel-air mixture is not derived to this region (see red color, Fig. 2).

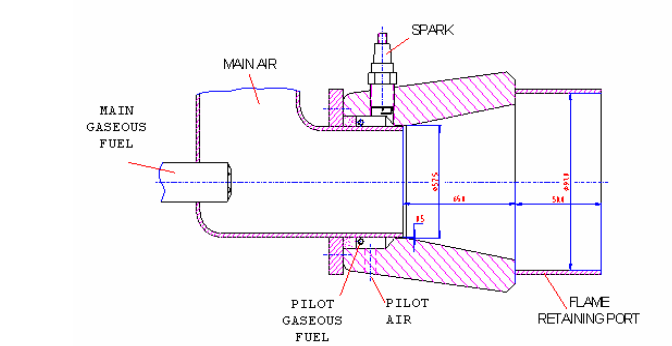

a)

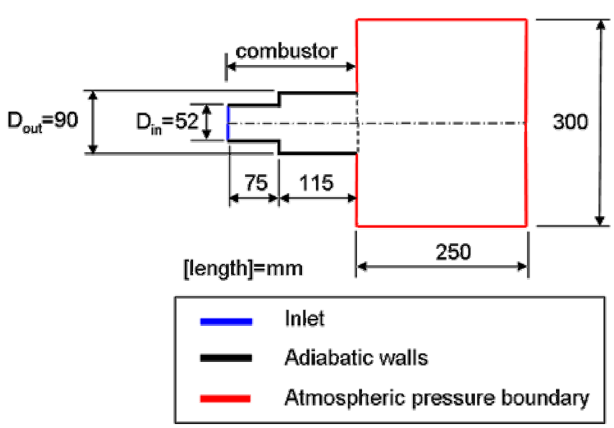

b)

Fig. 1 Schematic drawing for CFD modeling of the combustor unit, a)-actual combustor unit, b) CFD simulation model.

CHEMKIN MODEL

Values of fuel and air distribution are based on combustor drawings, on the given operating conditions and the CFD simulations. The pilot combustor, where rich gas-air mixture is burnt, was included in the simulation scheme and the effect of the pilot combustor parameters on combustion process was investigated. CHEMKIN 4.0 code with applications “AURORA” for “PSR” and “PLUG" reactors were used. For calculation of chemical reactions, the GRI-MECH Version 3.0 package with 325 reactions was used. A similar approach was tested and approved by shock-tube testing [15].

Residence time (τ) was estimated using CFD simulation results. The simulation model is shown in Fig. 3. The flame zone of the main combustor was split into ten sections; each section was represented by a perfectly stirred reactor (PSR). The residence time was assumed to be distributed equally between the reactors. The air and fuel flow rates distribution was obtained using the CFD simulation results. When examining Fig. 3 it is obvious that the flame is progressing and its volume is growing in the flow direction. In this exact manner the fresh fuel and air flow rates were set to the PSRs along the main combustor/flame axis: the first five PSRs received 5% of fresh mixture flow rate each, the next three PSRs received 10% each and the last two PSRs got as much as 25% each.

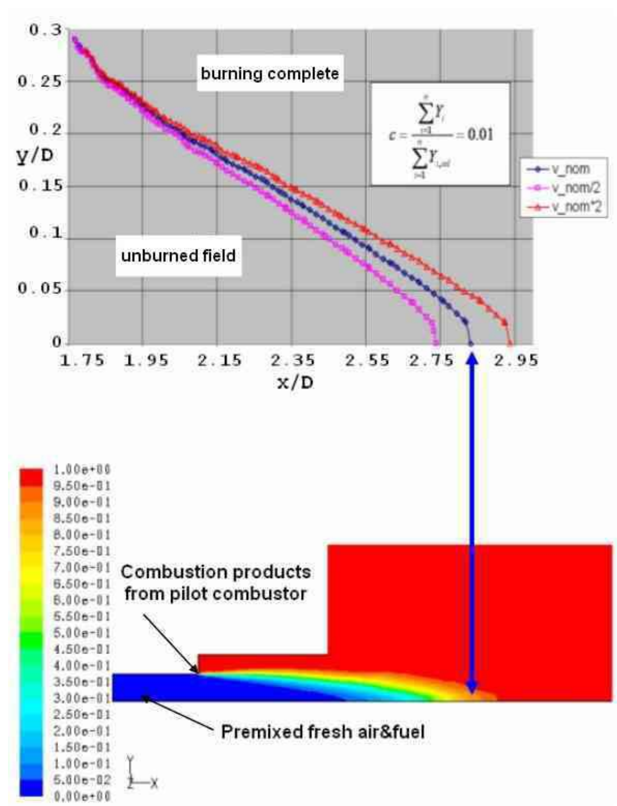

Fig. 2 Top: location (normalized to outlet diameter) of Flame Onset contours for different flow rates (nominal flow rate, half and double), ER_0 = 0.45; bottom: contours of progress variables, ***C*.**

It is important to mention that the recirculation zone, which existed in the CFD simulation (due to sudden expansion), does not exist in the final design (Fig. 1, top drawing). So the CHEMKIN model has no back-flow elements.

The flame stabilization effect exists due to a pilot combustor and the gradual addition of fuel and air mixture to the subsequent PSRs. The above-mentioned dispensation of the fresh mixture to the PSRs was also affected the need to match the flame temperature level to the temperature which resulted from the CFD simulation. It is clear that such approach incorporates arbitrary discretization, however it was assumed that it could be effective to obtain qualitative information about the effects of different parameters. For given values of air and fuel flow rates and air speed, the characteristic time, τ, was chosen to equal 20 msec. The simulation model and correspondence between CFD and CHEMKIN models is shown in Fig. 3. The combustion took place at PSRs1-10. The rich mixture was delivered to PSR1 and lean fuel-air mixture, with equal equivalence ratio, for the remaining reactors (PSRs 2-10). The equivalence ratio of the PSRs with lean mixture was calculated in such a way that the global equivalence ratio was kept the same for simulation cases where the pilot operated under rich condition and when it was operated under lean condition Each reactor had their fuel and air mass flow rates (in accordance with the CFD results). This simulated air and fuel supply from the inner unburned zone. The quantitative values were obtained from the burn out curves, based on results from the CFD simulation .

A portion of the combustion products were delivered to PSRs11-15 where reactions continued but without the addition of fresh air and fuel. This row of the reactors simulates the outer zone.

At the combustor exit, combustion products from the two rows of the reactors were mixed and delivered to PSR16 and then were directed to a plug flow reactor (PFR). According to the CHEMKIN model the CO emission concentration after PSR16 was three orders of magnitude larger than in experiments. A PFR was used to simulate the completion of the CO and UHC burnout process, with consequent CO concentration reduction without significant change in the outlet temperature. It should be noted that due to all approximations involved (such as not accounting for heat losses and gas-air mixture pre heating, usage of averaged velocities distributions and more), the chemical reaction network scheme is only capable to give qualitative results.

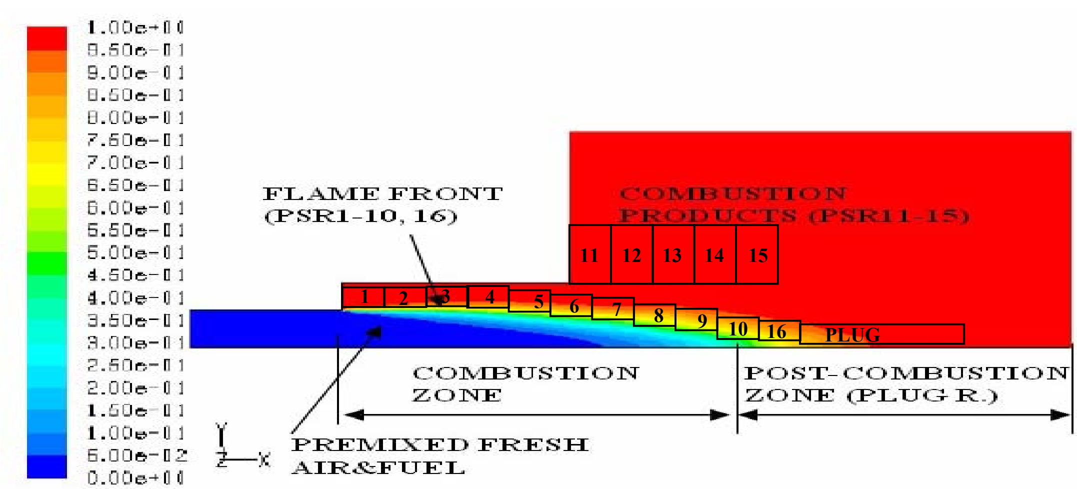

a)

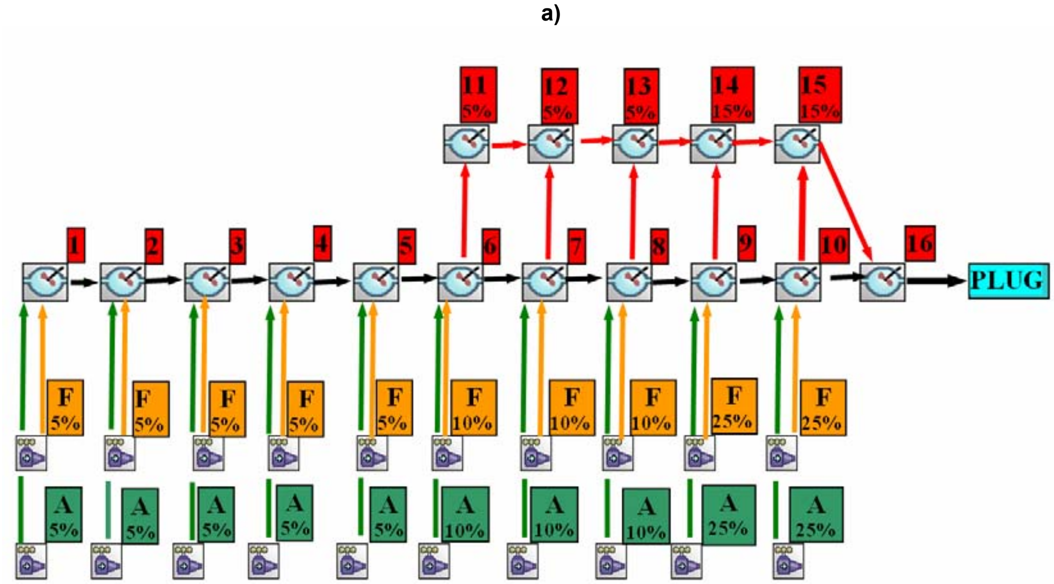

b)

Fig. 3 Scheme of combustion for CHEMKIN simulations (A-air, F- fuel, %-percent of mass flow rate of the main combustor); a) scheme of reactors location; b) network for CHEMKIN simulation.

The following cases were compared to verify the effectiveness of the proposed combustion technique:

1. Lean uniform mixture for all reactors PSR 1-10, see Table 1.
2. Rich mixture composition for the PSR-1 and lean – for PSR-2-PSR-10 for the same global ER as it is in 1, Table 2.
3. Rich mixture composition for the PSR-1 and lean – for PSR-2-PSR-10; global ER is the minimal value which provides stable combustion, Table 3.

Table 1. Simulation results of the "lean pilot" combustion. Conditions: T_{ad} =1,472K; ER_0 (R1-R16)=0.496; Tair=300K; Pair=1bar.

	Reactor 1	Reactor 16	Plug reactor
T,K	1,360	1,458	1,466
OH, ppm	662	493	53
CH3 ppm	55	53	0
H, ppm	154	10	0.01
O, ppm	363	97	1
CO, ppm	9,299	666	0.8
NO, ppm	0.2	0.6	0.7

Table 2. Simulation results of the "rich pilot" combustion. Conditions: T_{ad}=1,472K; ER_0=0.496; ER_1 (R1) =1.5; ER_2 (R2-16) = 0.48; Tair=300K; Pair=1bar.

	Reactor 1	Reactor 16	Plug reactor
T,K	1,860	1,441	1,468
OH, ppm	229	56	55
CH3, ppm	1,236	11	0
H, ppm	955	0.6	0.01
O, ppm	19	1.2	1
CO, ppm	74,880	3,602	0.9
NO, ppm	17.0	3.5	3.6

Table 3. Simulation results of the "rich pilot" combustion. Conditions: T_{ad}=1,421K; ER_0=0.469; ER_1 (R1) =1.5; ER_2 (R2-16) = 0.454; Tair=300K; Pair=1bar.

	Reactor 1	Reactor 16	Plug reactor
T,K	1,860	1,386	1,420
OH, ppm	229	44	41
CH3, ppm	1,236	19	0
H, ppm	955	0.4	0.006
O, ppm	19	0.5	0.7
CO, ppm	74,880	4,563	1
NO, ppm	17.0	2.4	3

Comments to the Tables: ER_1 - for the pilot combustor, ER_2 - for the main combustor, ER_0 - global,

Comparison of Tables 1 and 2 show that the use of pilot combustor increases NOx emission. In spite of the significant temperature and CO difference in intermediate stations, the temperature and CO values after plug reactor are close. Tables 2 and 3 also show that "rich" mixture in the pilot combustor increases NOx emission. This NOx enhancement is caused by high temperature after the pilot combustor.

Nevertheless, the most important result of these simulations is that it is possible to achieve stable combustion with low global ER (0.469 with "rich pilot", in comparison to ER value of 0.496 with "lean pilot"). It should be noted that the use of the conventional, diffusion based, pilot flame for stabilization of the whole combustor leads to far larger NO_x emission.

Temperature and main components evolution along the "central" row of reactors, for cases 1 and 3 (reactors 1-10, 16), are presented in Figs. 4-7. It can be seen that following reactor #1, all radicals have higher concentrations values in rich ER pilot combustor, however, most of them (CH3, H, O) are sharply reduced with time. In contrast, the OH radical has a longer lifetime. It seems that these radicals have significantly effect on combustion process and hence, they have an important role for improving combustion stability.

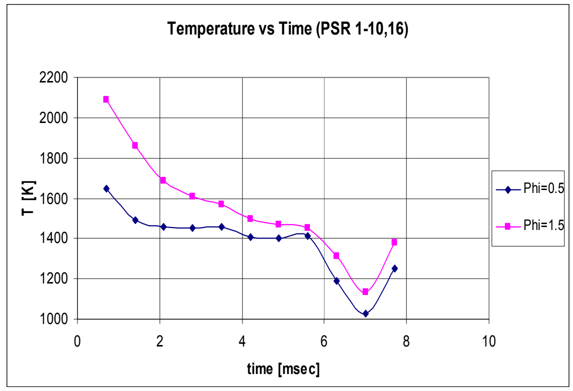

Fig. 4 Temperature evolution along the experimental combustor.

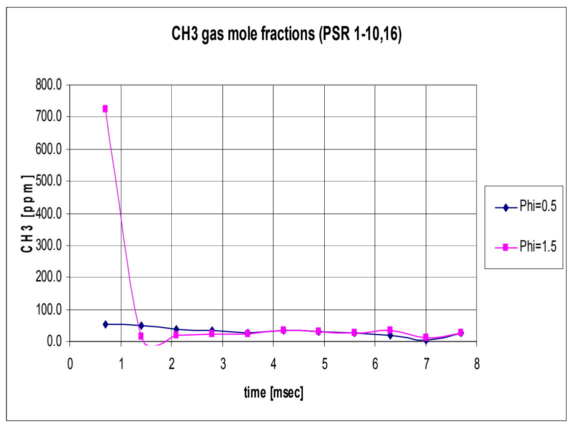

Fig. 5 CH_3 radical evolution along the experimental combustor.

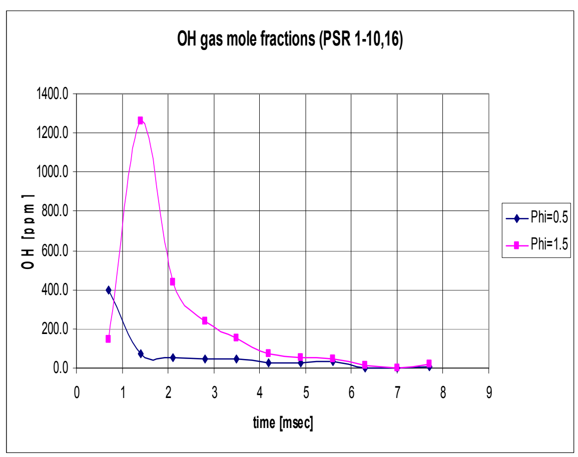

Fig. 6 OH radical evolution along the experimental combustor.

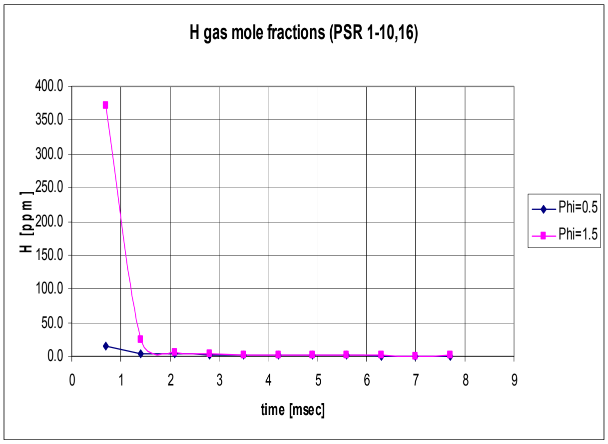

Fig. 7 H radical evolution along the experimental combustor.

Experimental study

EXPERIMENTAL SET-UP

The experimental setup was built and operated in order to compare experimental results with CFD and CHEMKIN simulations and to check for possible interactions between individual combustor within combustion system that is comprised of 4 identical combustor units; unit design is described above.

Figure 8 shows a general view of the combustor and experimental set-up. It includes 4 sets of separate pipe lines for air and fuel supply to the main and pilot combustors, following the mass flow measurements. Fuel lines for each pilot and main combustor had regulating valves for fine control of the fuel mass flow rate for each of the combustors. The temperature is measured by an open junction thermocouples, four thermocouples were installed inside two units located in an opposite diameter of the common combustor. Combustion products composition was measured by Horiba gas analyzer. Spectroscopic measurements were also performed and their details are described below.

Example of combustor operation under low ER is shown in Fig. 9.

Test results and discussion

TEMPERATURE DISTRIBUTION AND COMBUSTION PRODUCTS CONTENT

Most of tests were carried out for 3 different ERs in the pilot and main combustors, i.e. a collection of experiments represented by a 3X3 matrix tests was carried out (Table 4). Therefore different values of ERs for the pilot combustor provided very rich fuel, moderate rich fuel, and lean fuel. The main combustor ERs were close to blow out, and were between 0.5 and 0.6. We also tried to test the combustor under higher ERs but due to very high combustion temperature (temperature was outside high limit of thermocouples) only one point was tested (point 10, Table 4). The following parameters were measured:

- temperatures distribution along combustor length (thermocouples, 4 points. Thermocouples were located at distances that equaled to 120, 240, 350, 460 mm downstream of the pilot combustor exit cross section, see Fig. 8).
- combustion products composition (using Horiba gas analyzer). Data about CO and NO_x emissions were adjusted to 15% O_2 on dry basis at the exit as is in common practice for gas turbines.

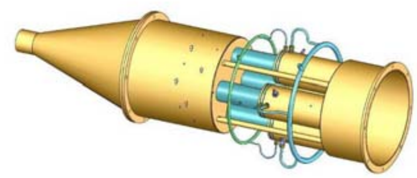

a)

b)

Fig. 8 Experimental combustor; a) general view, b) experimental set-up.

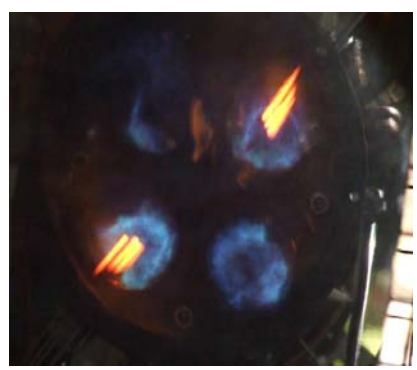

Fig. 9 Photograph of the combustor operation, global ER is equal to 0.51; yellow rods are thermocouples.

Table 4. Principal test results

#	ER_1	ER_2	ER_0	$T_1[^oC]$	$T_2[^oC]$	$T_3[^oC]$	$T_4[^oC]$	CO $[ppm]$	NO_X $[ppm]$
1	0.72	0.49	0.50	600	821	862	844	54.0	4.2
2	0.71	0.51	0.51	783	914	886	842	6.3	7.3
3	0.73	0.54	0.55	998	1,044	1,045	985	2.3	12.0
4	1.43	0.49	0.50	634	869	883	853	33.3	4.1
5	1.42	0.51	0.52	778	916	884	841	1.8	7.5
6	1.45	0.53	0.54	954	1,033	985	925	3.0	13.3
7	2.15	0.49	0.51	690	877	885	852	12.1	6.4
8	2.14	0.51	0.53	798	922	890	844	1.7	8.4
9	2.18	0.57	0.59	987	1,059	1,003	988	6.4	17.0
10	0.72	0.78	0.77	1,206	1,200	1,137	1,074	77.4	40.8

Comments to the Table:
ER_1- for the pilot combustor,
ER_2- for the main combustor,
ER_0 - global,
$T_1 - T_4[^oC]$ - Temperature measurements by thermocouples along combustor axis (at the above mentioned locations from the pilot to exit)

The effects of the pilot and main combustors ERs on NO_x emission values are shown in Fig. 10**.** It can be seen that NO_x increases with ER of the pilot as well as of the main combustor. The main reason is temperature increase as it is known that high temperature is the main factor for NO_x generation.

The maximum CO emission is observed for the lowest ER_2, (ER_2=0.5); this emission significantly decreases when ER_1 increases, see Fig. 11; hence, higher ER_1 values provide better burning conditions.

Temperature distribution is shown in Fig. 12. Maximum temperature is achieved at 240 mm downstream of the pilot combustor exit; temperature increases with ER. The effect of ER of the pilot combustor on temperature is significant for the case where the ER of the main combustor is low, Fig. 12c.

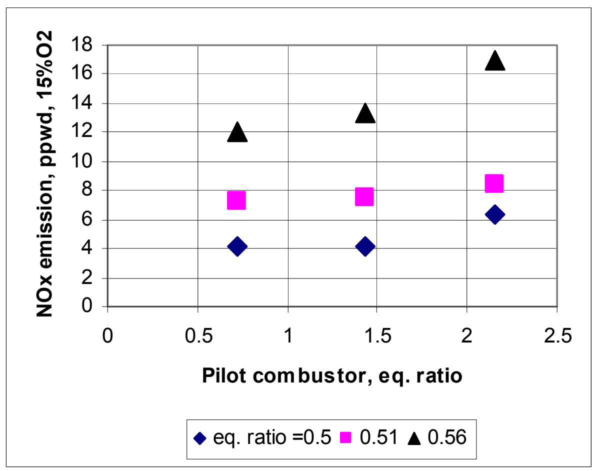

Fig. 10 Effect of ER of pilot combustor on NO_x emission for different ER of main combustor.

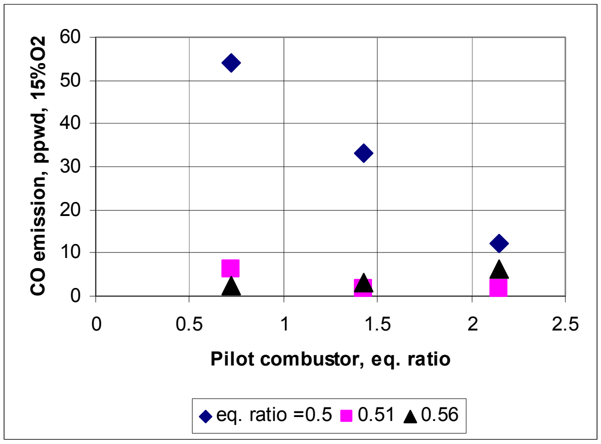

Fig. 11 Effect of ER of pilot combustor on CO emission for different ER of main combustor.

It is important to note that measured temperature values were lower than theoretical ones, mainly due to significant heat loss (non insulated system, hence convection and radiation), however the trends of the observed physical phenomena were as expected and according to theory.

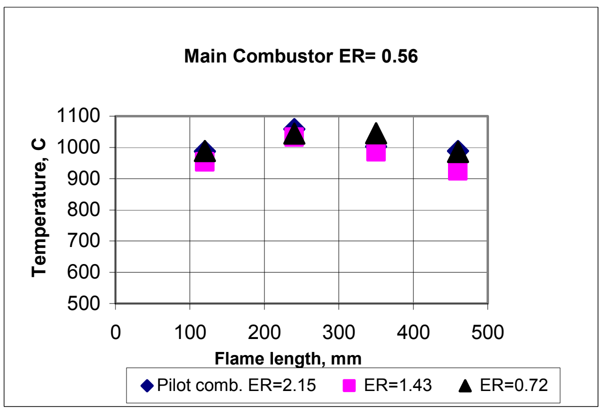

a)

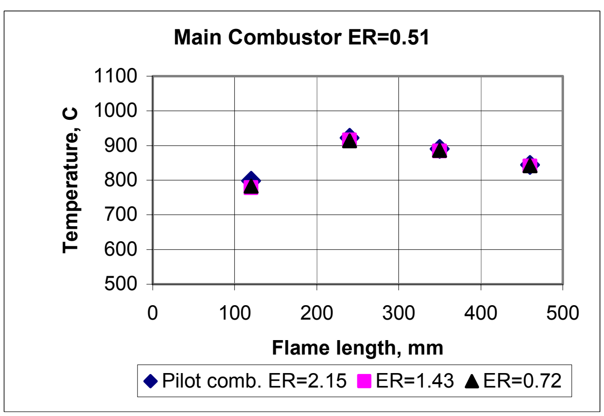

b)

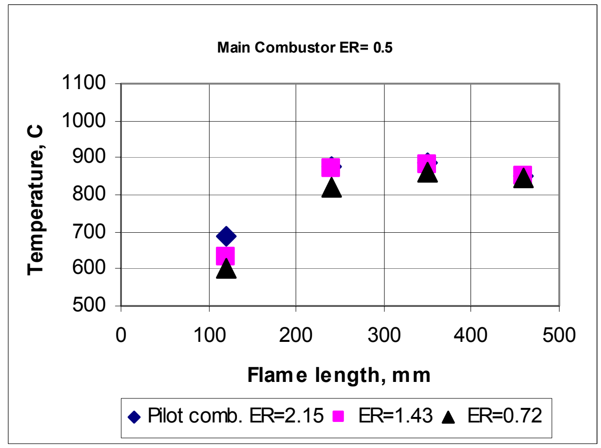

c)

Fig. 12 Temperature distribution along flame length (X-axis) for different ERs.

It should be pointed out that stable combustion was achieved for low values of global ER and this correlates well with simulation results. Effect of ER of the pilot combustor on temperature distribution is shown in Fig. 13. As expected, the higher the ER is the high temperature is observed, especially for small distances downstream the pilot combustor exit. This, together with radical generation, promotes stable combustion.

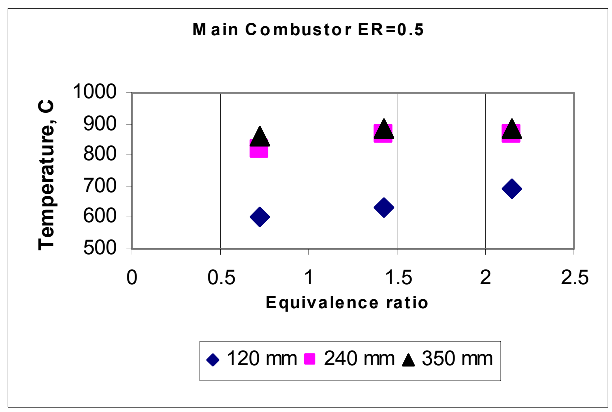

Fig. 13 Effect of ER of pilot combustor on combustion temperature (flame length, X-axis = varia).

The interaction between individual combustor units was not observed. Change of combustion regime in one unit does not effect on other ones.

SPECTROMETRIC MEASUREMENTS

Spectrometric measurements of the chemiluminescence through a quartz optical window were performed to detect free radicals. The emission in the ultraviolet and visible ranges was recorded with the aid of a fiber-optic based spectrometer. Local measurements of the emissions of the Swan bands of C_2* molecules at 471 nm, 513 nm, 560 nm, vibronic band of OH* radicals at 310 nm and the vibronic band of CH* radicals at 431 nm were recorded along the combustor centerline, downstream the pilot combustor exit. The distance from the pilot combustor was the same as for temperature measurements, namely, 30, 60, 95, and 150 mm. These distances along the combustor corresponded to residence times (according to CHEMKIN simulations, Figs. 4-7) that equaled to 2, 4, 6.3, 10 msec respectively.

It can be seen that the relative amount of radicals depends on the ER inside the pilot combustor and on the distance downstream of the pilot combustor exit, Table 5 (Measurements through orifice 4 somehow did not indicate the presence of radicals so this point does not appear in the Table). Measurements were carried out for three values of ER of the pilot combustor, namely 0.7 and 1.4 and 2.2. Maximum values of radicals are observed for ER of the pilot combustor that equaled to 1.4. To avoid massive soot deposits on the quartz window, the radicals' measurements were performed while the main combustion air was supplied however without its fuel (main combustor did not operate).

It can be seen that emission intensity is correlated with CHEMKIN simulations, Fig. 6. Experimental data relate to the descending branch of the curve. Examples of the spectroscopic measurements are shown in Figs. 14, 15.

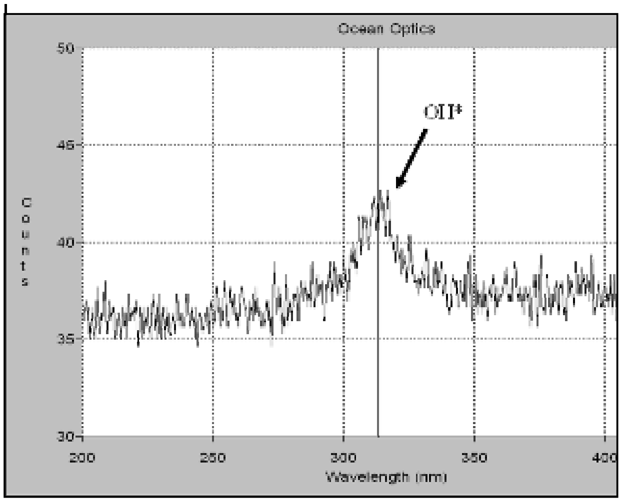

Fig. 14 Example of spectrometric measurements, ER_1 = 1.4; OH* radicals.

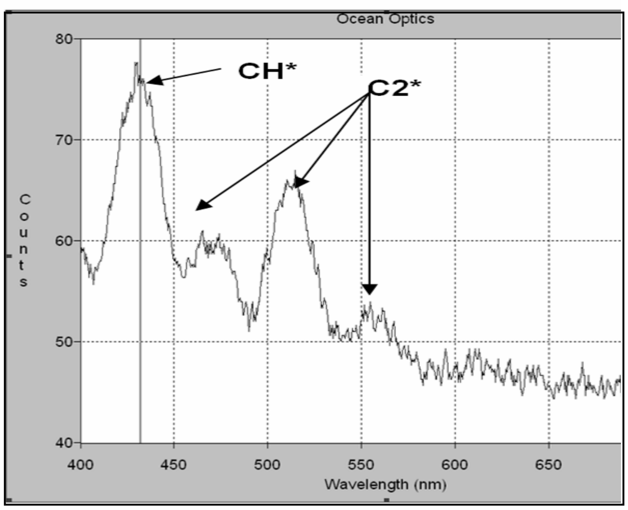

Fig. 15 Example of spectrometric measurements, ER_1= 1.4; C2* and CH* radicals.

CONCLUSIONS

1. Theoretical and experimental study of the effect of radical injection on the lower limit of stable combustion was carried out. The study was performed to improve understanding of the combustion process under realistic conditions. For this and for improved similarity with practical combustor of industrial gas turbine, a quad-combustor was, designed, manufactured and tested.

2. Computer simulations using Fluent and CHEMKIN codes showed evolution of radicals and other components of combustion products along flame length. Rich mixture conditions of the pilot combustor generates significantly more radicals than lean mixture and this lowers stable combustion boundary for lean premixed combustion.

3. Analysis of combustion products and temperature distribution along the combustor, were carried out for different ERs in the pilot and in the main combustors. The tests demonstrated low NO_x values at the exit. The lowest NO_x values were achieved for the "lean pilot" combustion with global ER_0=.0.496 (NO_x=0.7 ppm, Table 1). But the global lowest ER, ER_0=0.469, which still provides stable combustion was achieved for the pilot combustor with ER_1 = 1.5 (NO_x=3 ppm, Table 3). Thus, this value of NOx was only insignificantly increased in comparison with the case of "lean pilot" combustion in spite of the higher ER_1 of the "rich pilot" combustor.

Spectrometric measurements of the chemiluminescence demonstrated that rich mixture of the pilot combustor generates OH, CH*, C_2^* radicals. Maximum OH radical's emission correlates well with CHEMKIN simulations (correlates to the descending part of the curve, Fig. 6).

4. Theoretical study and experimental results shed light on the mechanism of stabilization using fuel rich pilot combustors, which can improve combustion stability operation of lean premixed GT combustors.

5. No significant interaction between the individual combustor units was observed.

Table 5 Spectral band intensity in counts for different distances downstream the pilot combustor exit

Pilot comb. ER_1	30 mm (2 msec)			60 mm (4 msec)				95 mm (6.3 msec)		
	OH*	CH*	C2*	OH*	CH*	C2*	Add	OH*	CH*	C2*
0.7	<1	<1 0	 0	0	0 0	 0		-	-	
1.4	5 34	 20	 13	3	0 <1	 0		0	0 0	 0
2.2	4 18	2 9	 7	1	0 0	 0	Wide band	0	0 0	 0

Upper values in a cell – data from UV spectra.
Lower values in a cell – data from VIS spectra.
Wide band – in VIS spectrum the broad band in range from 400nm to 850nm is measured

References

1. Lefebvre, A. H., "Gas Turbine Combustion", 2nd Edition, 1999, Taylor & Francis, Philadelphia.
2. Y.Levy, A. Gany, Y. Goldman, V. Erenburg, V. Sherbaum, V. Ovcharenko, L. Rosentsvit, B. Chudnovsky, A. Herszage, A. Talanker, INCREASING OPERATIONAL STABILITY IN LOW NO_X GT COMBUSTOR BY A PILOT FLAME, Proceeding of ASME Turbo Expo 2010: Power for Land, Sea and Air June 14-18, 2010, Glasgow, UK, GT2010-22785
3. Cabot, G., Vauchelles, D., Taupin, B., Boukhalfa, A., “Experimental study of lean premixed turbulent combustion in a scale gas turbine chamber”, Experimental Thermal and Fluid Science 28 (2004) pp. 683-690.
4. Lieuwen, T., Zinn, B.T., “The role of ER oscillations in driving combustion instabilities in low NO_x gas turbines”, 27th Symposium (Int.) on Combustion/The Combustion Institute (1998) pp. 1809-1816.
5. Schefer, R.W., Wicksall, D.M., Agrawal, A.K., “Combustion of hydrogen-enriched methane in a lean premixed swirl-stabilized burner”, Proceedings of the Combustion Institute 29 (2002) pp.843-851.
6. P. Albrecht,,S. Bade, A. Lacarelle, C. O. Paschereit, E. Gutmark, Instability Control by Premixed Pilot Flames, Journal of Engineering for Gas Turbines and Power APRIL 2010, Vol. 132 / 041501-1.
7. Barbosa, S., Garcia, M.L.C., Ducruix, S., Labegorre, B., Lacas, F., “Control of combustion instabilities by local injection of hydrogen”, Proceedings of the Combustion Institute 31 (2007) pp. 3207-3214.
8. Takita, K., Masuya, G., Sato, T., Ju, Y., “Effect of addition of radicals on burning velocity”, AIAA Journal, Vol. 39, No. 4 (2001) pp.742-744.
9. Ionov, V.G, “Study of separate stages of pre-chamber ignition by cinematographic analysis”, Combustion, Explosion, and Shock Waves, Vol. 26, No. 2 (1990) pp.129-133.
10. T. Bohen, Y. Goldman, A. Gany, D. Cohen, “Effect of free radicals on flame ignition”, 19th Annual Symposium of the Israeli Section of the Combustion Institute, December 25, 2003, pp.77-82.
11. D.Cohen, Master’s Thesis, Faculty of Aerospace Eng., Technion, Haifa, Israel and The University of Manchester, UK, 2004.
12. Y. Goldman, G. Conway and A. Gany, “Influence of Cold Free Radicals Injection on Combustor Ignition”, 46th Israel Annual Conference on Aerospace Sciences, Tel-Aviv and Haifa, March 1-2, 2006.
13. Fristrom, R.M., Westenberg, A.A., “Flame Structure and Processes”, The John Hopkins Institute, McGraw-Hill Book Company,1995.
14. Fluent 6 User's Guide, Fluent Inc., Lebanon, NH, 2001.
15. Y. Levy, E. Olchanski, V. Sherbaum, V. Erenburg, A. Burcat, “Shock Tube and Modeling Ignition study of Methane in air and Recirculated Combustion Products”, J. Propulsion and Power, No 3, 2006, pp.669-676.